The Iranian Journal of Mechanical Engineering Transactions of ISME
Journal homepage: https://jmee.isme.ir/
Vol. 24, No. 1, 2023, pp. 99-118

Research Paper

DOI: https://doi.org/10.30506/jmee.2023.540505.1276
DOR: https://dorl.net/dor/20.1001.1.16059727.2023.24.1.3.7

Elastoplastic Analysis of Rotating Disk of Variable Thickness Made of Functionally Graded Materials

Behrooz Shahriari*
Assistant professor

Mohammad Reza karamoozravari†
Associate professor

This paper is dealing with the Elastoplastic analysis of rotating disks of variable thickness made of functionally graded materials based on Tresca's yield criterion. To do so, the governing equations of rotating annular disks are established based on the elasticity theory. Then, using Tresca's yield criterion and the elastic-perfectly plastic flow law, the displacement equations and stresses are obtained in the plastic region. In order to find the effects of the shape of the disk profile on its stress distribution, the thickness of the disk cross-section is supposed to vary as an exponential function of the radius. In addition, considering different places at which the yielding starts, the process of expanding the plastic flow is investigated. The obtained results are validated against those reported for homogeneous as well as constant thickness FGM disks, showing good agreement. The findings also demonstrate that taking the variable thickness for the disk cross-section into account has a significant effect on the stress distribution and prediction of the place where the yielding initiate.

Keywords: Rotating disk, Elastoplastic analysis, Functionally graded materials, Tresca yield criterion

1 Introduction

In most engineering designs and analyzes; the equivalent stress is not allowed to exceed the elastic limit and applying the safety factor makes the situation worse, so that one cannot use the full capacity of a structure to withstand the applied loads. It means that the weight of the structure, costs construction, and in some cases fuel consumption would increase.
Rotating equipment, such as rotating disks, play a key role in various industries, i.e., aerospace, automotive, and marine, so that it is necessary to accomplish research on its various aspects. Recently, the applications of functionally graded materials in manufacturing the rotating disks have attracted great attention. These materials show gradual and continuous changes of composition, structure and properties in different directions of the piece.

---

* Corresponding Author, Assistant professor, Faculty of Mechanics, Malek Ashtar University of Technology, Iran, shahriari@mut-es.ac

† Associate professor, Department of Mechanical Engineering, Graduate University of advanced Technology, Kerman, Iran, m.karamooz@kgut.ac.ir

Received: 2021/10/15, Revised: 2022/12/21, Accepted: 2023/10/04

In 1925, László studied the elastoplastic behavior of a rotating disk and since then, this subject attracted the attention of other researchers [1]. However, more serious efforts in the field of elastoplastic is attributed to Gamer. He published four papers on the deformation and distribution of the elastoplastic stresses in a rotating disk with different boundary conditions using the Tresca's yield criterion and flow law. Gamer supposed a constant value for the disk density and thickness [1-4]. Güven investigated the effect of density on the elastoplastic stresses of a rotating annular disk of variable thickness [5] and under external pressure [6], considering Tresca's yield criterion and flow law. Rees compared the stress distribution of rotating disks on the basis of both Von Mises and Tresca's yield criterions and obtained a significant difference between these two [7]. You and Zhang presented a solution for elastoplastic of a solid-state disk using Von Mises yield criteria [8]. You et al., presented a numerical solution, based on Runge-Kutta numerical method, for a variable thickness and density rotating disk with a nonlinear hardness [9]. Eraslan and Orcan analyzed an elastoplastic tension of solid-state rotating disk of exponentially variable thickness and linear stiffness [10]. They presented an analytical solution using the Tresca's yield criterion, the linear flow, and linear strain hardening rule for elastoplastic deformation of a solid-state rotating disk [11]. In another work, they investigated the point at which the yielding initiates in a variable thickness annular disk [12]. Vullo and Vivio solved the equations of a rotating elastoplastic disk of variable-thickness and nonlinear strain hardening [13]. Toussi and Farimani analyzed the deformation in a rotating elastoplastic disk for velocities more than yielding limit. They investigated the effects of different parameters, including cross-sectional profiles and material properties, on the critical velocities of the disk [14]. Haghpanah et al., presented a numerical solution for the elastoplastic analysis of a rotating disk made of functionally graded materials of linear hardening [15]. Zamani Nejad et al., presented an accurate analytical elastoplastic solution for a constant thickness rotating disk made of functionally graded material [16]. Lomakin et al. analyzed the elastoplastic strain fields of an annular rotating disk using the Von Mises' yield criterion in conjunction with the flow law [17]. Thawait et al. presented an elastic analysis of functionally graded variable thickness rotating disk by element-based material grading [18]. The results of that work showed that there is a significant reduction of stresses in functionally graded material disks as compared to homogeneous disks and the disks modeled by power law functionally graded material have better strength. A finite-difference method is used to obtain the thermal elastic-plastic stresses and strains for a rotating annular disk by Sharma and Sanehlata [19]. In that work, the disk was made of functionally graded materials whose thickness decreases exponentially and density increases exponentially with non-linear strain hardening behavior. An analysis of propagation of elastic-plastic front of functionally graded rotating disk under centrifugal and thermal load in post-elastic regime has been done by Nayak et al. [20]. In that work the modeling of functionally graded materials has been done using power law variation of volume fraction. Semka et al. analyzed the use of various piecewise linear and smooth plasticity functions and flow theory to solve the rotating disk problem and to compare the determined displacement and deformation fields for the selected plasticity functions [21]. In that work, it has been proved that the Tresca yield condition can be employed to solve problems similar to the rotating disk problem. Sharma et al. studied thermoelastic characteristics in the functionally graded material rotating disk with the help of a finite element method under exponentially and linearly varying material properties along radius of disk [22]. Kholdi et al. presented a thermo-elasto-plastic analysis of a rotating disk made of functionally graded materials using successive approximation method [23]. They have investigated effects of angular speed, percentage of ceramic particles, particle reinforcement power, and boundary conditions on radial and tangential thermo-elasto-plastic strains, stresses, and equivalent stresses.

To the best of the authors' knowledge, there is a lack of comprehensive study of the elastoplastic response of variable thickness functionally graded annular disks.

In the present paper, this deficiency is tried to be fulfilled. To do so, variable thickness functionally graded circular annular disks are taken into account in conjunction with Tresca's yield criterion in order to study the elastoplastic response. Figure (1) shows a schematic representation of the problem under consideration, and the geometrical and loading main parameters. In this figure, a and b are respectively the inner and outer radius, and ω the angular velocity.

2 Governing equations

As shown in figure (1), there is a circular annular rotating disk at an angular velocity of $\boldsymbol{\omega}$ with the internal radius of $\boldsymbol{a}$ and external radius of $\boldsymbol{b}$ made of functionally graded materials that is sufficiently thin and large. According to the geometry of the problem, formulation and review of results in a cylindrical coordination is performed and presented. The thickness of the disk cross section, the elastic modulus, the density, and the yielding tension are assumed to be in the form of power-law functions of the radial coordinate, as presented by equation (1).

$$
\begin{aligned}
h(r) &= h_0\left(\frac{r}{b}\right)^{\delta_t n} \\
E(r) &= E_0\left(\frac{r}{b}\right)^{\delta_E n} \\
\rho(r) &= \rho_0\left(\frac{r}{b}\right)^{\delta_\rho n} \\
\sigma_Y(r) &= \sigma_{Y_0}\left(\frac{r}{b}\right)^{\delta_\sigma n}
\end{aligned}
\tag{1}
$$

in which h_0, E_0, ρ_0 and σ_{Y_0} are the thickness, modulus of elasticity, density, and yield stress at the outer radius, $r = b$, respectively.δ_t, δ_E, δ_ρ and δ_σ denote some constant values, and n is the power parameter. If the properties presented by equation (1) are generally denoted by P and its value in the outer radius by P_0, the variation of the dimensionless property, i.e., $\bar{P} = {P}/{P_0}$, can be depicted as a function of dimensionless radius, $\bar{r} = r/b$, as shown in figure (2).

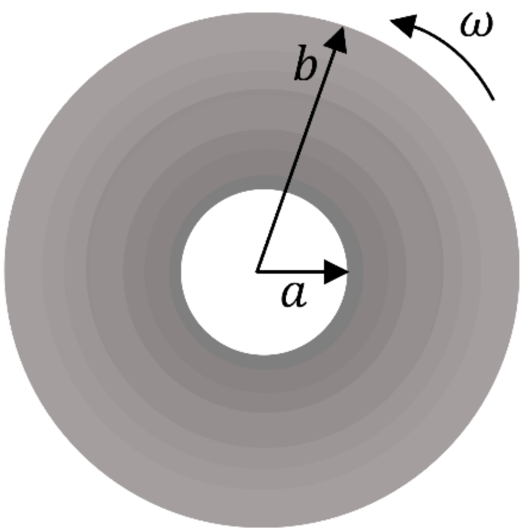

Figure 1 Schematic representation of a FGM disk and its main parameters

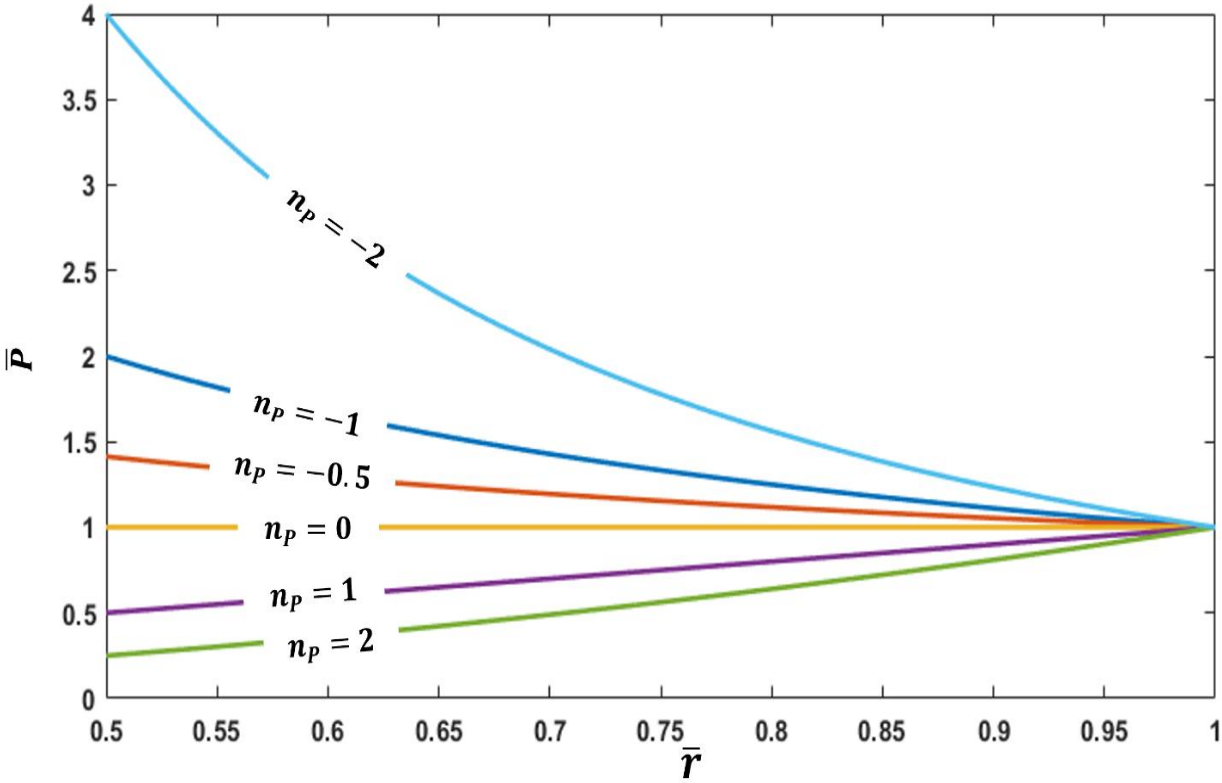

Figure 2 Variation of an arbitrary dimensionless geometrical or material property $\bar{P}$, as a function of the dimensionless radius $\bar{r}$

2.1 Elastic Behavior Analysis

The equilibrium equation of the rotating disk considering the thickness effect is given by equation (2):

$$\frac{d}{dr}(hr\sigma_r) - h\sigma_\theta + h\rho\omega^2 r^2 = 0 \tag{2}$$

in which σ_r and σ_θ are the components of radial and circumferential stresses. It should be noted that body force due to the weight (ρg) is neglected. The radial and peripheral displacements are considered as u and v, respectively. Regarding axisymmetric assumption, there is no circumferential change so that v = 0. Therefore, the strain-displacement relations in the cylindrical coordinates are equal to:

$$\begin{gathered} \varepsilon_r = \frac{du}{dr} \\ \varepsilon_\theta = \frac{u}{r} \\ \gamma_{r\theta} = 0 \end{gathered} \tag{3}$$

in which ε_r is the radial strain, ε_θ the circumferential strain, and $\gamma_{r\theta}$ the shear strain. Using Hooke's law for the plane stress state and substitution of strain-displacement relations presented in equation (3), the stress relationship in term of radial displacement is given by:

$$\sigma_r = \frac{E(r)}{1-\nu^2}\left(\frac{du}{dr} + \nu\frac{u}{r}\right)$$
$$\sigma_\theta = \frac{E(r)}{1-\nu^2}\left(\frac{u}{r} + \nu\frac{du}{dr}\right) \tag{4}$$

where ν is the Poisson ratio. Using the stress components presented by equation (2), the equilibrium equation of the disk might be expressed by equation (5):

$$r^2\frac{d^2u}{dr^2} + (n_E + n_t + 1)r\frac{du}{dr} + ((n_E + n_t)\nu - 1)u$$
$$= -\frac{1-\nu^2}{E_0}\rho_0 b^{n_E-n_\rho}\omega^2 r^{(n_\rho-n_E+3)} \tag{5}$$

Hereafter, the parameters $n_t = \delta_t n$, $n_E = \delta_E n$, $n_\rho = \delta_\rho n$, and $n_\sigma = \delta_\sigma n$ are used in order to simplify the derived equations. The analytic solution of the second-order differential equation of (5), in term of displacement, has the generalized form as:

$$u = -Ar^{m_3} + C_1 r^{m_1} + C_2 r^{m_2} \tag{6}$$

Where C_1 and C_2 denote integration constants., and A, m_1, m_2, and m_3 parameters can be formulated as follows:

$$A = \frac{\left(\frac{1-\nu^2}{E_0}\right)\rho_0 b^{n_E-n_\rho}\omega^2}{n_\rho(n_\rho+6) + (\nu - n_\rho - 3)n_E + (n_\rho - n_E + 3 + \nu)n_t + 8}$$
$$m_1 = \frac{-(n_E+n_t) + \sqrt{(n_E+n_t)^2 - 4((n_E+n_t)\nu - 1)}}{2} \tag{7}$$
$$m_2 = \frac{-(n_E+n_t) - \sqrt{(n_E+n_t)^2 - 4((n_E+n_t)\nu - 1)}}{2}$$
$$m_3 = n_\rho - n_E + 3$$

By substituting equation (6) into (4), the radial and circumferential stresses can be obtained using the following equation:

$$\sigma_r = \frac{E(r)}{1-\nu^2}\left[-A(m_3+\nu)r^{(m_3-1)} + (m_1+\nu)C_1 r^{m_1-1} + (m_2+\nu)C_2 r^{m_2-1}\right]$$
$$\sigma_\theta = \frac{E(r)}{1-\nu^2}\left[-A(m_3\nu+1)r^{m_3-1} + (m_1\nu+1)C_1 r^{m_1-1} + (m_2\nu+1)C_2 r^{m_2-1}\right] \tag{8}$$

Constants C_1 and C_2 can be obtained from the specified boundary conditions. For an annular disk, radial stress at the inner radius $(\sigma_r)_{r=a}$ and outer one $(\sigma_r)_{r=b}$ is zero. Consequently, applying the boundary conditions for an annular disk, the constants C_1 and C_2 are obtained as:

$$C_1 = \frac{\left(a^{m_2} b^{(3)} - a^{m_3} b^{m_2+n_E-n_\rho}\right) R}{(m_1+\nu)(a^{m_2} b^{m_1} - a^{m_1} b^{m_2})}$$
$$C_2 = \frac{(a^{m_3-1} b^{n_E-n_\rho+m_1-1} - a^{m_1-1} b^{(2)}) R}{(m_2+\nu)(a^{m_2-1} b^{m_1-1} - a^{m_1-1} b^{m_2-1})} \tag{9}$$

where R denotes a constant parameter which can be expresses by equation (10).

$$R = \frac{(m_3+\nu)\left(\frac{1-\nu^2}{E_0}\right)\rho_0\omega^2}{n_\rho(n_\rho+6)+(\nu-n_\rho-3)n_E+(n_\rho-n_E+3+\nu)n_t+8} \tag{10}$$

In order to obtain a general solution, the following dimensionless parameters are taken into account:

$$\bar{u} = \frac{uE_0}{\sigma_{Y_0} b} \qquad \Omega = \left(\frac{\rho}{\sigma_{Y_0}}\right)^{1/2} b\omega \qquad \bar{r} = \frac{r}{b}$$
$$\bar{\sigma}_r = \frac{\sigma_r}{\sigma_{Y_0}} \qquad \bar{\sigma}_\theta = \frac{\sigma_\theta}{\sigma_{Y_0}} \qquad \bar{a} = \frac{a}{b} \tag{11}$$
$$\bar{C}_1 = \frac{C_1 E_0 b^{m_1-1}}{\sigma_{Y_0}} \qquad \bar{C}_2 = \frac{C_2 E_0 b^{m_2-1}}{\sigma_{Y_0}}$$

2.2 Investigation of yielding initiation

To obtain the angular velocity corresponding to the yield threshold and investigation of the yield conditions, the Tresca's yield criterion has been used. To do so, the principal stresses must be obtained. On the other hand, the order of the main tensions (σ_r and σ_θ in this problem) depends on the numerical value of the exponential parameters n_t, n_E, n_ρ, n_σ and the ratio of radii (r/b). Therefore, referring to reference [16], to monitor the start of yielding, the dimensionless variable Ψ has been used. This variable is based on Tresca's criterion and is defined as:

$$\Psi(\bar{r}) = \bar{r}^{(-n_\sigma)} Max\{(\bar{\sigma}_\theta - \bar{\sigma}_r), (\bar{\sigma}_\theta), (\bar{\sigma}_r)\} \tag{12}$$

The above criterion states that yield starts at a point at which Ψ has its highest value, i.e., Ψ=1. To analyze the behavior of a rotating disk made of functionally graded materials, depending on the value of power parameters, the yield may start from inner radius, outer radius, simultaneously at inner and outer radius or somewhere in between.

2.2.1 Initiation of the yielding from the inner radius

Yield begins from the inner radius when $\Psi(\bar{a}) = 1$ and function Ψ at the inner radius is of the highest absolute value. Using the stresses expressed by equation (8) and the boundary condition as $(\bar{\sigma}_r)_{\bar{r}=\bar{a}} = 0$, the non-dimensional critical angular velocity, Ω_{e1}, is obtained as:

$$\begin{aligned}\Omega_{e1} = \{S[&-(m_1+\nu)(m_2+\nu)(m_3\nu+1)(\bar{a}^{m_2}-\bar{a}^{m_1})\bar{a}^{(m_3)} + (m_1\nu \\ &+ 1)(m_2+\nu)(m_3 \\ &+\nu)(\bar{a}^{m_2}-\bar{a}^{m_3})\bar{a}^{m_1} \\ &+(m_2\nu+1)(m_1+\nu)(m_3+\nu)(\bar{a}^{m_3}-\bar{a}^{m_1})\bar{a}^{m_2}]^{-1}\}^{0.5}\end{aligned} \tag{13}$$

where S and H are constant parameters presented by equations (14) and (15), respectively:

$$S = \frac{(1-\nu^2)(m_1+\nu)(m_2+\nu)(\bar{a}^{m_2}-\bar{a}^{m_1})}{H(\bar{a})^{n_E-n_\sigma-1}} \tag{14}$$

$$H = \frac{(1-\nu^2)}{n_\rho(n_\rho+6)+(\nu-n_\rho-3)n_E+(n_\rho-n_E+3+\nu)n_t+8} \tag{15}$$

2.2.2 Initiation of the yielding from outer radius

In this case, the yield begins at the outer radius where the function Ψ has the highest absolute value, i.e., $\Psi(1) = 1$. Using the stress components and the specified boundary condition as $(\bar{\sigma}_r)_{\bar{r}=\bar{b}} = 0$, the non-dimensional critical angular velocity, Ω_{e2}, is obtained as presented by equation (16):

$$\begin{aligned}\Omega_{e2} = \{S_b[&-(m_1+\nu)(m_2+\nu)(m_3\nu+1)(\bar{a}^{m_2}-\bar{a}^{m_1})+(m_1\nu+1)(m_2+\nu)(m_3+\nu)(\bar{a}^{m_2}-\bar{a}^{m_3}) \\ &++(m_2\nu+1)(m_1+\nu)(m_3+\nu)(\bar{a}^{m_3}-\bar{a}^{m_1})]^{-1}\}^{0.5}\end{aligned} \tag{16}$$

where the constant S_b is defined as:

$$S_b = \frac{(1-\nu^2)(m_1+\nu)(m_2+\nu)(\bar{a}^{m_2}-\bar{a}^{m_1})}{H} \tag{17}$$

2.2.3 Simultaneous yield at the inner and outer radius

In this case, the yield starts simultaneously at the inner and outer radius, where the function Ψ is of its highest value, i.e., $\Psi(\bar{a}) = 1$ and $\Psi(1) = 1$. Regarding the boundary conditions of the disk and using relations (13) and (16), the critical dimensionless angular velocity of the rotating disk, Ω_{cr}, and the critical power parameter, n_{cr}, are obtained by solving equation (18):

$$\begin{cases} \Omega_{cr} - \{S_a[-(m_1+\nu)(m_2+\nu)(m_3\nu+1)(\bar{a}^{m_2}-\bar{a}^{m_1})\bar{a}^{(m_3)} \\ +[\![(m]\!]_1\nu+1)(m_2+\nu)(m_3+\nu)(\bar{a}^{m_2}-\bar{a}^{m_3})\bar{a}^{m_1} \\ +(m_2\nu+1)(m_1+\nu)(m_3+\nu)(\bar{a}^{m_3}-\bar{a}^{m_1})\bar{a}^{m_2}]^{-1}\}^{0.5}=0 \\ \\ \Omega_{cr} - \{S_b[-(m_1+\nu)(m_2+\nu)(m_3\nu+1)(\bar{a}^{m_2}-\bar{a}^{m_1}) \\ +(m_1\nu+1)(m_2+\nu)(m_3+\nu)(\bar{a}^{m_2}-\bar{a}^{m_3}) \\ +(m_2\nu+1)(m_1+\nu)(m_3+\nu)(\bar{a}^{m_3}-\bar{a}^{m_1})]^{-1}\}^{0.5}=0 \end{cases} \quad (18)$$

2.2.4 Initiation of yielding at some place between inner and outer radius

Considering r_{ep} as the radial position of the points at which the initiation of yielding occurs, the following relations are valid.

$$\begin{cases} \Psi(\bar{r}_{ep})=1 \\ \left.\dfrac{d\Psi}{dr}\right|_{\bar{r}=\bar{r}_{ep}}=0 \end{cases} \quad (19)$$

For a power parameter n, the required rotational angular velocity to start the plastic flow and the starting point of the yield is calculated by equation (19).

2.3 Analysis of Plastic Behavior

In this section, the stresses are always considered to be arranged in such a way that $\sigma_\theta > \sigma_r > \sigma_z = 0$. Accordingly based on the Tresca's criterion, $\sigma_\theta^P = \sigma_Y$ is considered. Substituting σ_Y into the equilibrium equation (2) implies the following differential equation:

$$\frac{d}{dr}(hr{\sigma_r}^P) = h{\sigma_Y}_0(\frac{r}{b})^{n_\sigma} - h\rho\omega^2r^2 \quad (20)$$

Solving the first-order linear differential equation (20) yields:

$${\sigma_r}^P = {\sigma_Y}_0 b^{-n_\sigma}\left(\frac{r^{n_\sigma}}{n_\sigma+n_t+1}\right) - \rho_0 b^{-n_\rho}\omega^2(\frac{r^{(n_\rho+2)}}{n_t+n_\rho+3}) + C_3 r^{(-n_t-1)} \quad (21)$$

In this relation, C_3 denotes the integrating constant that can be calculated according to the boundary conditions. Dimensionless shapes of stresses in the plastic region, $\bar{\sigma}_\theta^P$ and $\bar{\sigma}_r{}^P$, are as:

$$\begin{gathered} \bar{\sigma}_\theta^P = (\bar{r})^{n_\sigma} \\ \bar{\sigma}_r{}^P = \left(\frac{(\bar{r})^{n_\sigma}}{n_\sigma+n_t+1}\right) - (\frac{\Omega^2}{n_t+n_\rho+3})\bar{r}^{(n_\rho+2)} + \bar{C}_3\bar{r}^{(-n_t-1)} \end{gathered} \quad (22)$$

where $\bar{C}_3$ is defined as:

$$\bar{C}_3 = \frac{C_3}{\sigma_{Y_0} b^{n_t+1}} \tag{23}$$

According to the plastic flow law and the stress state ($\sigma_\theta > \sigma_r > \sigma_z = 0$), $\varepsilon_r^P = 0$ is considered. Taking the constant volume law in the plastic region into account, i.e., $\varepsilon_r^P + \varepsilon_\theta^P + \varepsilon_z^P = 0$, one would have $\varepsilon_\theta^P = -\varepsilon_z^P$. The total strain in any direction is the sum of elastic strain and plastic strain in that direction:

$$\begin{gathered} \varepsilon_r = \varepsilon_r^e \\ \varepsilon_\theta = \varepsilon_\theta^e + \varepsilon_\theta^p \end{gathered} \tag{24}$$

where superscripts e and p respectively denote the elastic and plastic part of the strain. Using the strain-displacement relations, the Navier equation in the plastic region is obtained as:

$$\begin{aligned} \frac{du}{dr} = \frac{1}{E_0}\left(\frac{r}{b}\right)^{-n_E} \Bigg[& \sigma_{Y_0}\left(\frac{r}{b}\right)^{n_\sigma}\left(\frac{1}{n_\sigma + n_t + 1} - \nu\right) - \rho_0 b^{-n_\rho}\omega^2\left(\frac{r^{(n_\rho+2)}}{n_t + n_\rho + 3}\right) \\ & + C_3 r^{(-n_t-1)} \Bigg] \end{aligned} \tag{25}$$

Solving equation (25), the displacement in the plastic region implies:

$$\begin{aligned} u^p = \frac{1}{E_0}\Bigg[& \frac{\sigma_{Y_0} b}{n_\sigma - n_E + 1}\left(\frac{r}{b}\right)^{n_\sigma - n_E + 1}\left(\frac{1}{n_\sigma + n_t + 1} - \nu\right) \\ & - \frac{\rho_0 \omega^2 b^3}{(n_t + n_\rho + 3)(n_\rho - n_E + 3)}\left(\frac{r}{b}\right)^{n_\rho - n_E + 3} + \frac{C_3 b^{n_E}}{(-n_t - n_E)} r^{(-n_t - n_E)}\Bigg] \\ & + C_4 \end{aligned} \tag{26}$$

where C_4 is a constant of integration. The dimensionless form of displacement in the plastic region might be expressed as:

$$\begin{aligned} \bar{u}^p = \Bigg[& \frac{1}{n_\sigma - n_E + 1}\bar{r}^{n_\sigma - n_E + 1}\left(\frac{1}{n_\sigma + n_t + 1} - \nu\right) \\ & - \frac{\Omega^2}{(n_t + n_\rho + 3)(n_\rho - n_E + 3)}\bar{r}^{n_\rho - n_E + 3} + \frac{\bar{C}_3}{(-n_t - n_E)}\bar{r}^{(-n_t - n_E)}\Bigg] \\ & + \bar{C}_4 \end{aligned} \tag{27}$$

Where

$$\bar{C}_4 = \frac{C_4}{\sigma_{Y_0} b^{n_t+1}} \tag{28}$$

3 Results

In this section, the results obtained from the analysis of yield threshold of a rotating annular disk of variable thickness made of functionally graded materials are presented. In this research changes in the Poisson ratio are considered to be negligible so that a constant value of 0.3 is supposed throughout the paper. Radial ratio is considered to be $\bar{a}$ = 0.5. Before investigating the effect of various parameters on the onset of yielding of a rotating disk, the proposed approach is validated. To do so, first the radial stress, $\bar{\sigma}_r$, as well as circumferential stress, $\bar{\sigma}_\theta$, corresponding to the critical angular velocity of a homogeneous annular disk with a constant thickness is investigated and the obtained results are compared with those reported in [12]. As shown in Fig. 3, it can be concluded the accuracy of the results of the analysis. It is worthwhile noting that for a homogeneous constant thickness rotating disk, the yielding always starts at the inner radius. In figure (4), the critical angular velocity at which yielding starts at the inner and outer radius is depicted with respect to $\bar{a}$. Referring to this figure, $\Omega_{e2} > \Omega_{e1}$ for all values of $\bar{a}$. As a result, for a homogeneous constant thickness annular disk the onset of yielding occurs at the inner radius.

Figure (5) shows the critical angular velocity at which a homogeneous variable thickness disk yields at its inner and outer radius with respect to the dimensionless radius $\bar{a}$. The power parameter n_t = -1 is considered. As shown in figure (5), for all values of the dimensionless radius, $\bar{a}$, one has $\Omega_{e2} > \Omega_{e1}$. Table (1) compares the critical angular velocities at the dimensionless inner radius of $\bar{a}$ = 0.5.

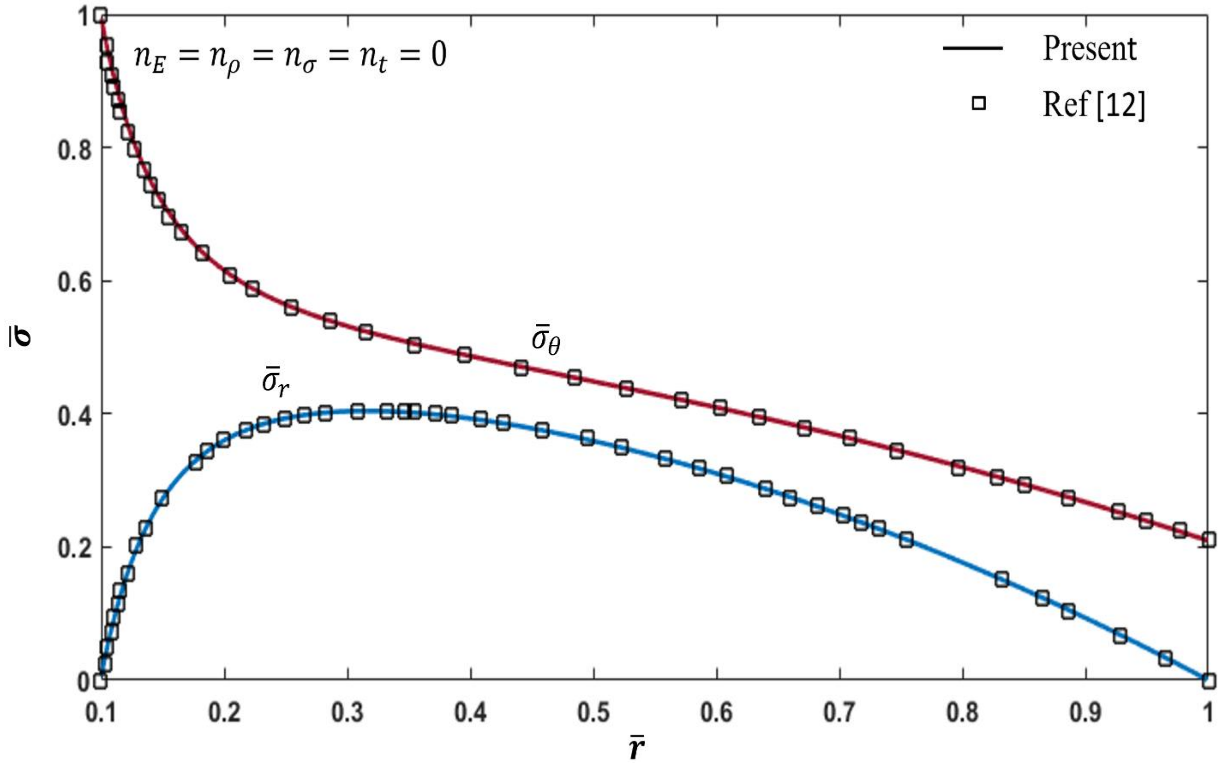

Figure 3 Dimensionless stress components of a constant thickness rotating disk as a function of dimensionless radius at the elastic limit angular velocity of $\boldsymbol{\Omega = 1.094351}$

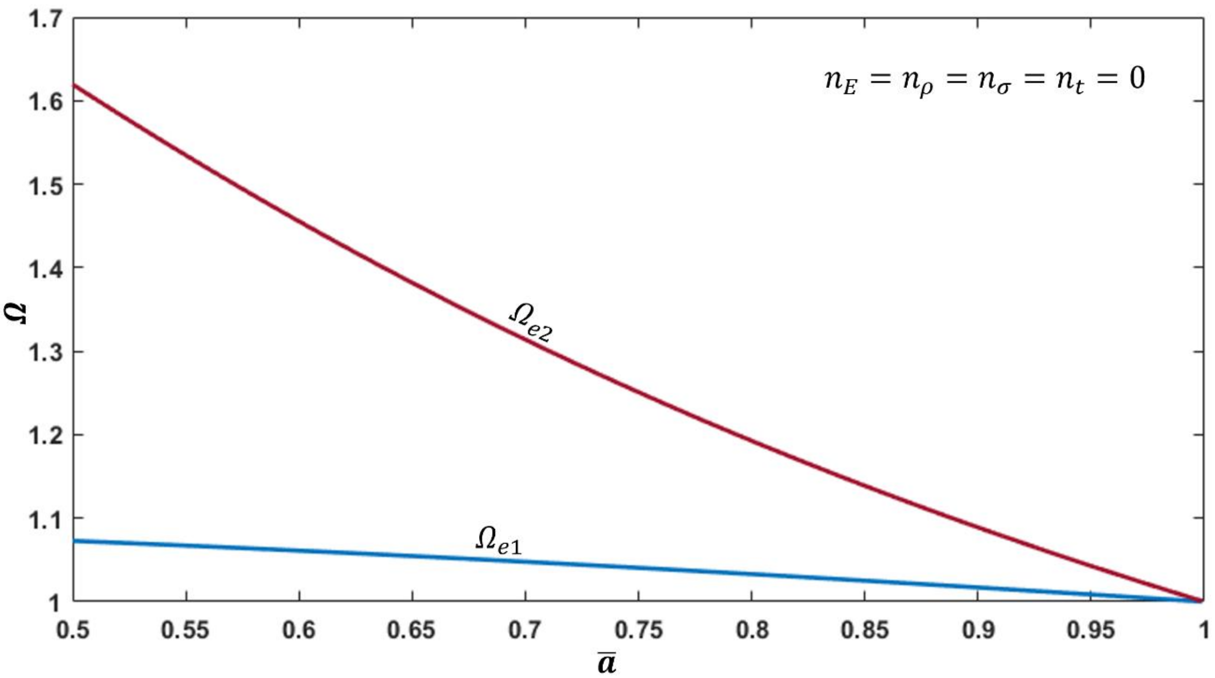

Figure 4 The variation of the critical angular velocity for the onset of yielding at inner and outer radius versus the dimensionless inner radius $\bar{\boldsymbol{a}}$, for a constant-thickness homogeneous disk

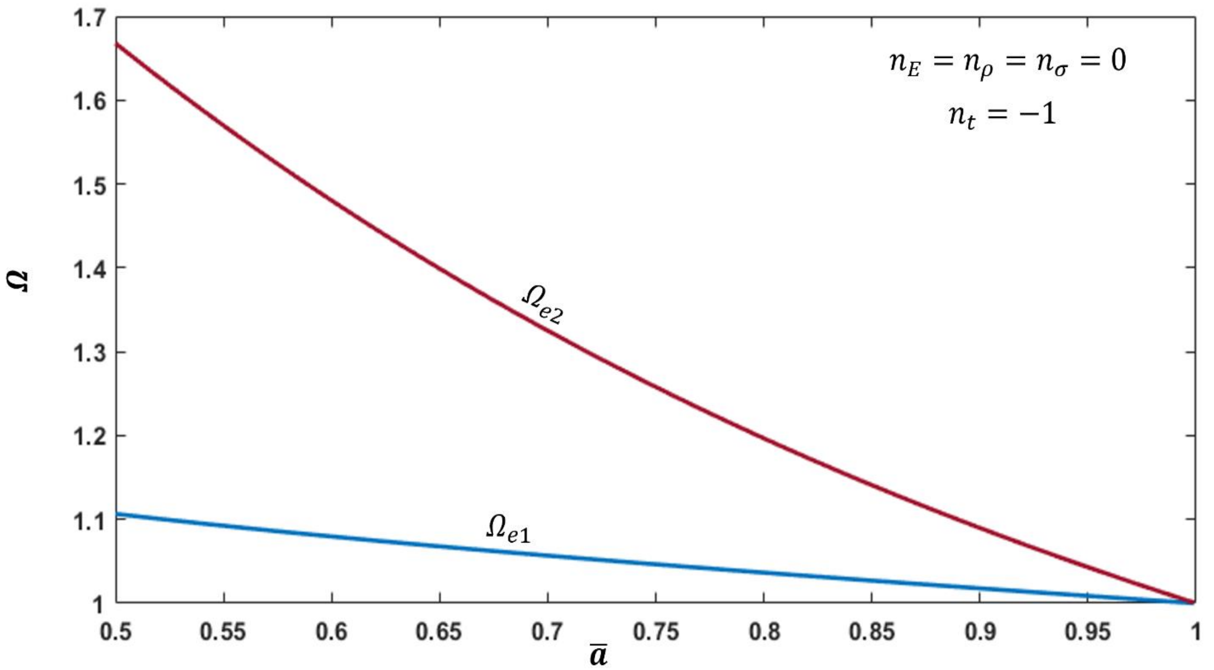

Figure 5 The variation of the critical angular velocity for the onset of yielding at inner and outer radius versus the dimensionless inner radius $\bar{\boldsymbol{a}}$, for a variable-thickness homogeneous disk.

Table 1 Dimensionless terminal rotational speed $\boldsymbol{\Omega}$ in inner radius $\bar{\boldsymbol{a}} = \mathbf{0.5}$

power parameter n_t	critical angular velocity Ω_{e1}	critical angular velocity Ω_{e2}
$n_t = 0$	1.0729	1.6196
$n_t = -0.5$	1.1037	1.6678
$n_t = -1$	1.1418	1.7180

In the next step, the radial stress, $\bar{\sigma}_r$, the circumferential stress, $\bar{\sigma}_\theta$, and the dimensionless function, Ψ, with respect to the dimensionless radius, $\bar{r}$, of a rotating annular disk made of functionally graded materials for the fixed thickness state are reviewed. As shown in figure (6), the results are compared with those reported in [16]. Referring to this figure, the power parameter of $n = 0.7424$, critical angular velocity of $\Omega = 1.27165$, the dimensionless inner radius of $\bar{a} = 0.5$, and $\Psi = 1$ are taken into account, so that the yielding starts at the inner radius. The power constants are supposed to be as $\delta_t = 0$ and $\delta_E = \delta_\rho = 2\delta_\sigma = 2$. As shown in figure (6), the obtained results are consistent with the results reported in [16].

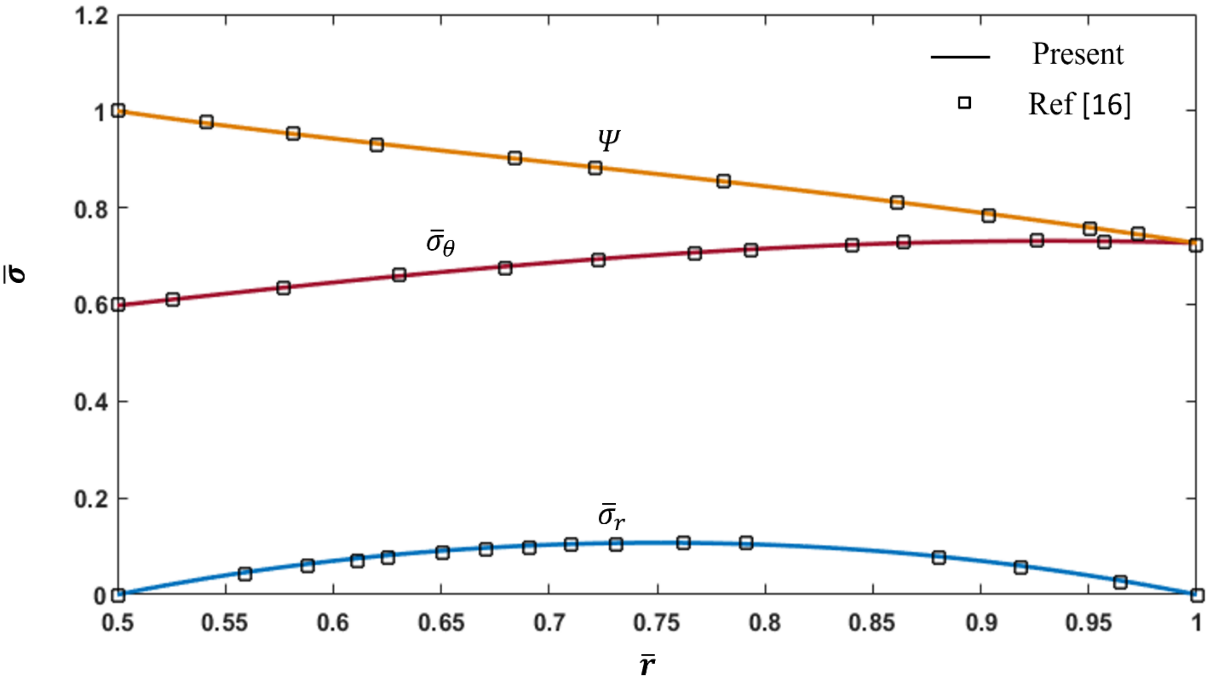

Figure 6 Variation of the radial stress, $\bar{\sigma}_r$, circumferential stress, $\bar{\sigma}_\theta$, and dimensionless function, Ψ, as a function of dimensionless radius, $\bar{r}$. The critical angular velocity of $\Omega_{e1} = 1.27165$ and the power parameter of $n = 0.7424$ are supposed.

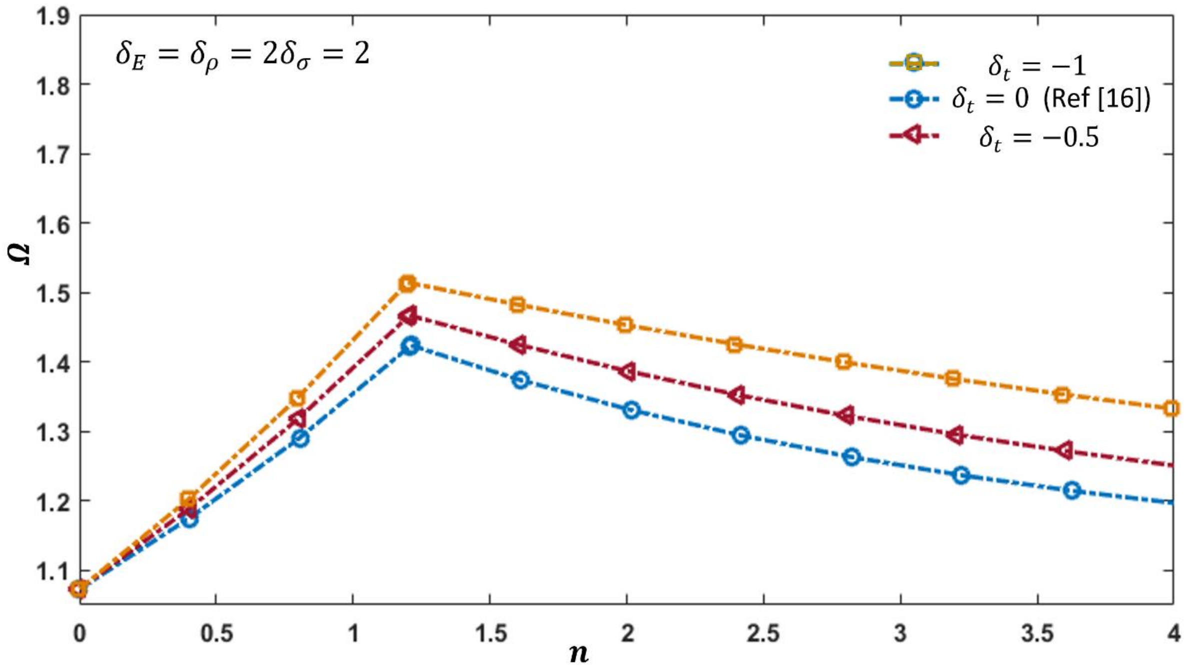

Figure 7 variation of the critical angular velocity versus the power parameter.

Figure (7) shows the effect of power parameter, n, on the non-dimensional angular velocity, Ω, at different thickness variations. As shown in this figure, increasing the value of δ_t, increases the critical angular velocity due to the reduction of the stresses. Table (2) shows the critical values of n and Ω for different values of δ_t which are obtained using figure (7). As might be seen, the value of the critical power, n_{cr}, slightly decreases when the thickness variation increases.

In order to determine the onset of yielding, some necessary and sufficient conditions must be satisfied. Table (3) summarizes the sufficient condition for the onset of yielding. The sufficient condition for the initiation of yielding is that the function Ψ takes the highest value at the starting point of yielding, otherwise, the plastic flow gets started at somewhere between the inner and outer radius.

The various modes of yielding initiation of a rotating annular disk of variable thickness made of functionally graded materials are considered. To provide numerical results, the constant values of the power, δ_i, are supposed to be as $\delta_E = \delta_\rho = 2\delta_\sigma = 2$ and $\delta_t = -0.5$. Figure (8) shows the variation of the stresses and function Ψ as a function of dimensionless radius for power parameter of n = 0.9 and a critical angular velocity of Ω = 1.3532. As can be seen, at the inner radius ($\bar{a}$ = 0.5), the Ψ function has its highest value, i.e., 1, so that the yielding starts at the inner radius of the disk.

In order to start yielding at the outer radius, the power parameter value of n = 1.8 and the critical angular velocity of Ω = 1.4055 are taken into account. As shown in figure (9), at the outer radius ($\bar{r}$ = 1), the value of Ψ =1 is achieved, so that the yielding begins at the outer radius.

For emphasizing the importance of the sufficient condition, the variation of the dimensionless function Ψ in terms of dimensionless radius $\bar{r}$ for $n = n_{\mathrm{cr}}$ and $\Omega = \Omega_{cr}$ is depicted in figure (10). Referring to this figure, at the inner and outer radius, the value of $\Psi = 1$ is reached. However, the highest value of the function is at a point between the inner and outer radius, which means the yielding happens at some place in between.

As already shown, the starting point of yielding is determined according to the values of the power parameter and the critical angular velocity. When the angular velocity increases to the values higher than the critical one, the region where the plastic deformation occurs would extend. As previously shown, a homogeneous disk starts to yield at its inner radius. Regarding the continuity of the disk, the displacement as well as stresses must be equal at the elastoplastic boundary. Accordingly, the following boundary conditions might be applied in order to obtain the unknown constants of the elastic and plastic regions as well as the radius of the elastoplastic region r_{ep}:

$$\begin{cases} \bar{\sigma}_r^e(\bar{r}_{ep}) = \bar{\sigma}_r^p(\bar{r}_{ep}) \\ \bar{\sigma}_\theta^e(\bar{r}_{ep}) = \bar{\sigma}_\theta^p(\bar{r}_{ep}) \\ \bar{u}^e(\bar{r}_{ep}) = \bar{u}^p(\bar{r}_{ep}) \\ \bar{\sigma}_r^e(1) = 0 \\ \bar{\sigma}_r^p(\bar{a}) = 0 \end{cases} \tag{30}$$

Table 2 Critical values of non-dimensional angular velocity, $\boldsymbol{\Omega}$, and power parameter, $\boldsymbol{n}$, for different values of $\boldsymbol{\delta_t}$.

δ_t	n_{cr}	Ω_{cr}
0	1.2109	1.4236
−0.5	1.2055	1.4669
−1	1.1995	1.5141

Table 3 The necessary conditions for onset yield

place of getting started to yielding	power parameter n	rotational speed Ω
inside radius	$n < n_{cr}$	$\Omega_{e1} < \Omega_{e2}$
outside radius	$n > n_{cr}$	$\Omega_{e1} > \Omega_{e2}$
simultaneously from inside radius and outside	$n = n_{cr}$	$\Omega_{e1} = \Omega_{e2}$

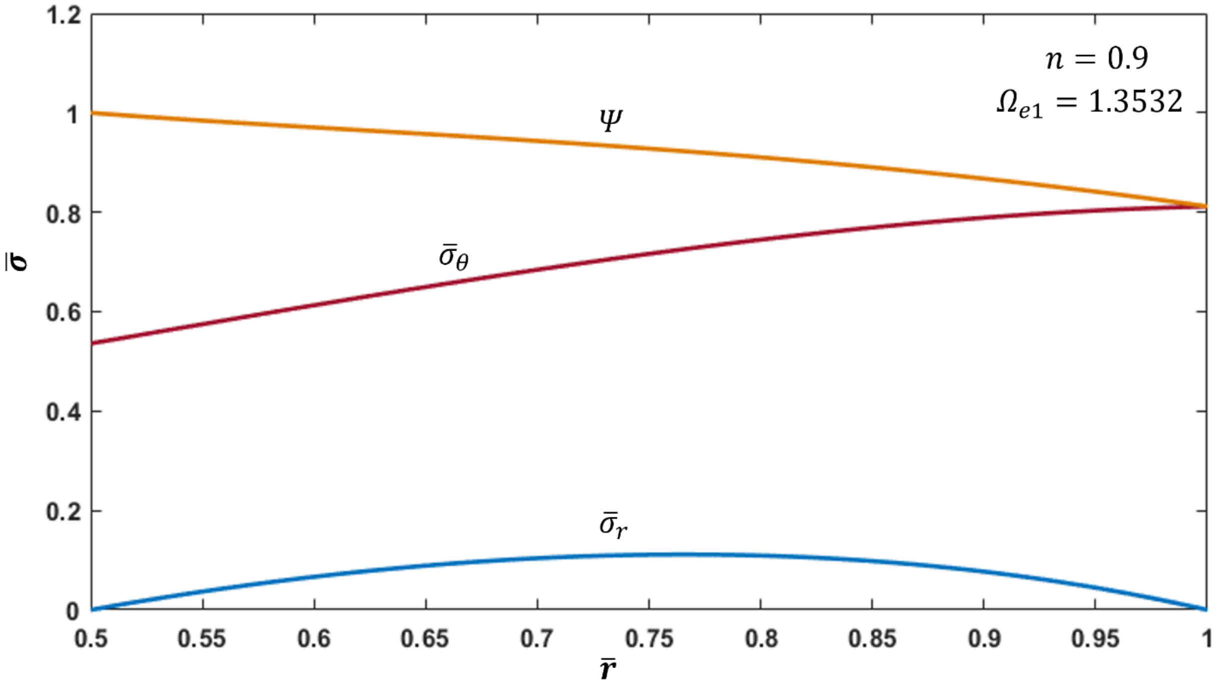

Figure 8 Variation of Radial stress $\boldsymbol{\bar{\sigma}_r}$, circumferential stress $\boldsymbol{\bar{\sigma}_\theta}$ and dimensionless function, $\boldsymbol{\Psi}$ as a function of dimensionless radius $\boldsymbol{\bar{r}}$ for the critical angular velocity of $\boldsymbol{\Omega_{e1} = 1.3532}$ and the power parameter of $\boldsymbol{n = 0.9}$.

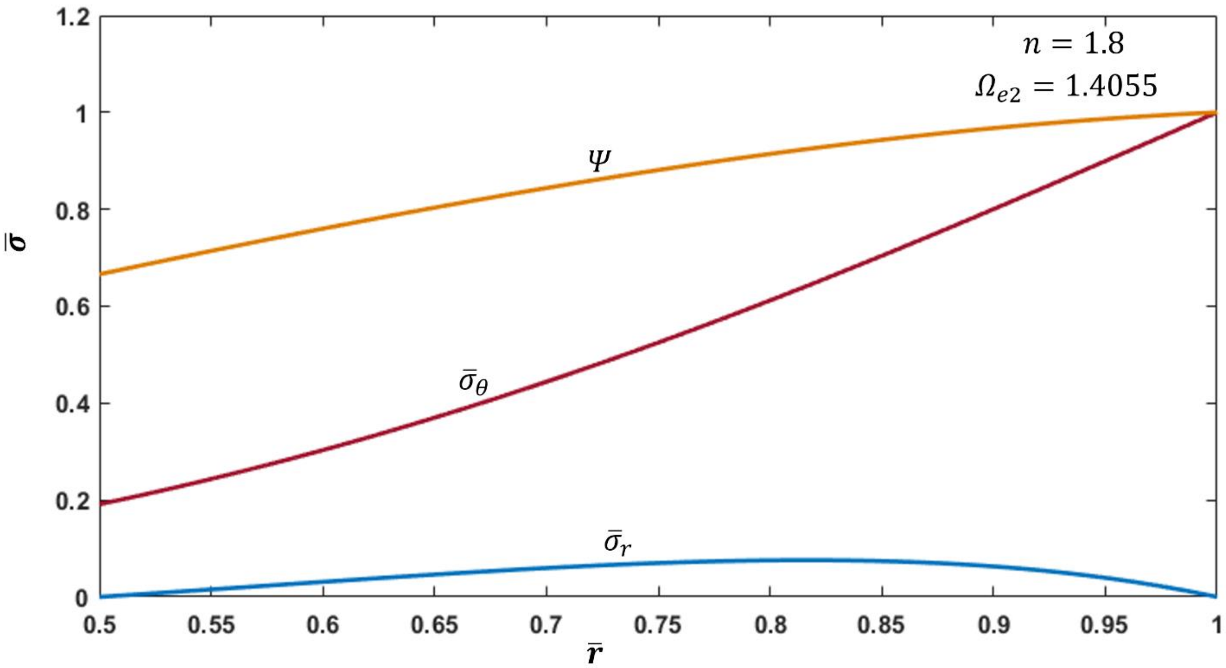

Figure 9 Variation of Radial stress $\boldsymbol{\bar{\sigma}_r}$, circumferential stress $\boldsymbol{\bar{\sigma}_\theta}$ and dimensionless function, $\boldsymbol{\Psi}$ as a function of dimensionless radius $\boldsymbol{\bar{r}}$ for the critical angular velocity of $\boldsymbol{\Omega_{e2} = 14055}$ and the power parameter of $\boldsymbol{n = 1.8}$.

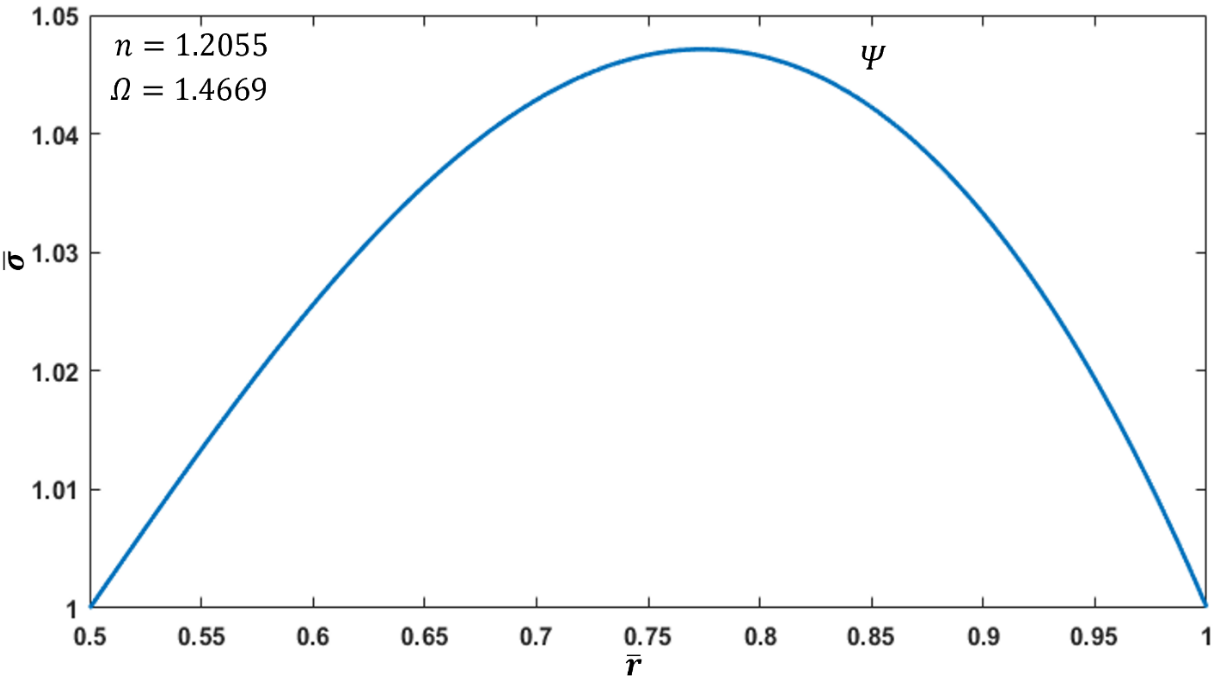

Figure 10 Variation of dimensionless function, $\boldsymbol{\Psi}$ as a function of dimensionless radius, $\bar{\boldsymbol{r}}$, for the critical speed of $\boldsymbol{\Omega_{cr}} = \mathbf{1.4669}$ and the power parameter of $\boldsymbol{n} = \mathbf{1.2055}$.

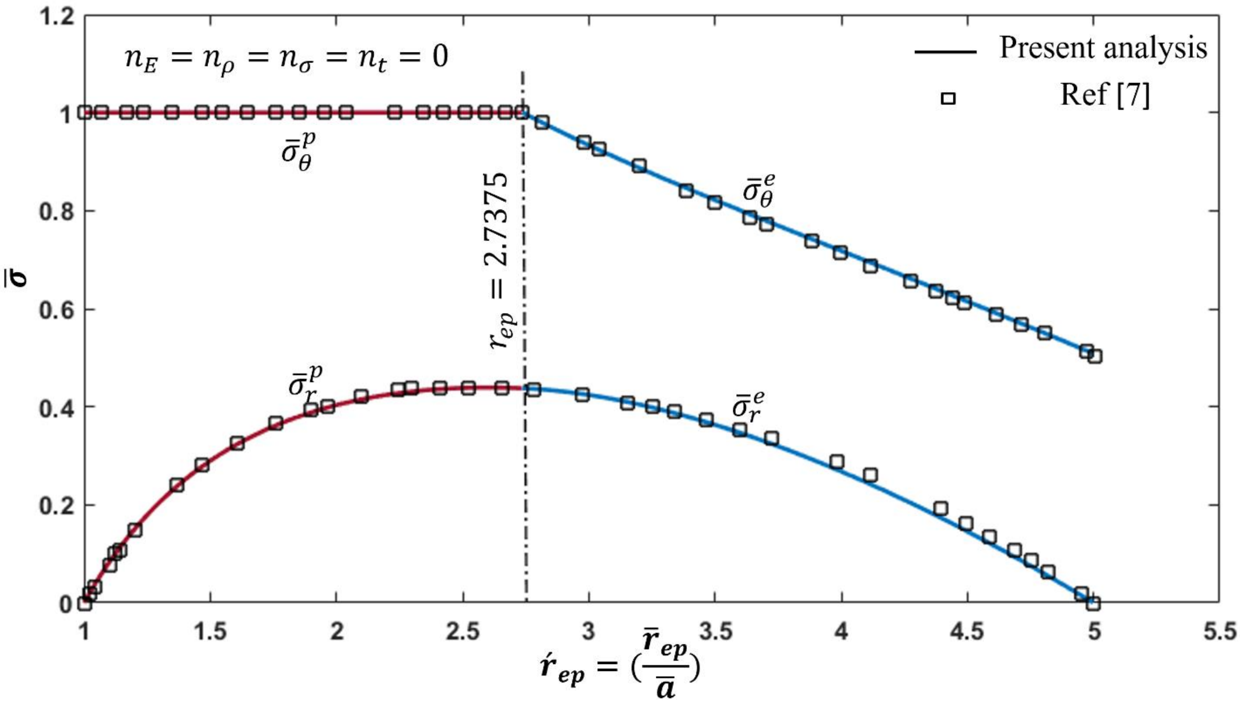

Figure 11 Variation of the radial stress, $\bar{\boldsymbol{\sigma}}_{\boldsymbol{r}}$, and circumferential stress, $\bar{\boldsymbol{\sigma}}_{\boldsymbol{\theta}}$, as a function of dimensionless radius, $\acute{\boldsymbol{r}}_{\boldsymbol{ep}}$, for the angular velocity of $\boldsymbol{\Omega} = \mathbf{1.44}$

Figure (11) shows the progression of the plastic region of a homogeneous disk, for ν= 0.28 and the inner dimensionless radius $\bar{a} = 0.2$. As can be seen, at a critical angular velocity of $\Omega = 1.44$, the boundary of the plastic region extends to the dimensionless radius of r_{ep} = 2.7375. The results are also consistent with those reported in [18].
As shown in figure (12), the progression of the plastic region for a rotating disk made of functionally graded materials with a fixed thickness (n_t = 0), is investigated., and the obtained results are compared with those reported in [16]. For power parameter of n = 0.7424 and angular

velocity of Ω =1.34, the boundary of the plastic region extends from inner radius to the dimensionless radius of r_{ep} = 0.735. As can be seen, the results are in geed agreement with those reported in [16].
Figure (13) shows the progression of the plastic region for a rotating disk made of functionally graded materials with variable thickness. For the power parameter n = 0.9 and the angular velocity of Ω =1.39, the boundary of the plastic region extends from the inner radius to the dimensionless radius of r_{ep} = 0.7313. Table (4) shows the unknown constants, C_{I}, obtained in the elastic and plastic regions as well as the radius of the elastoplastic region r_{ep}.

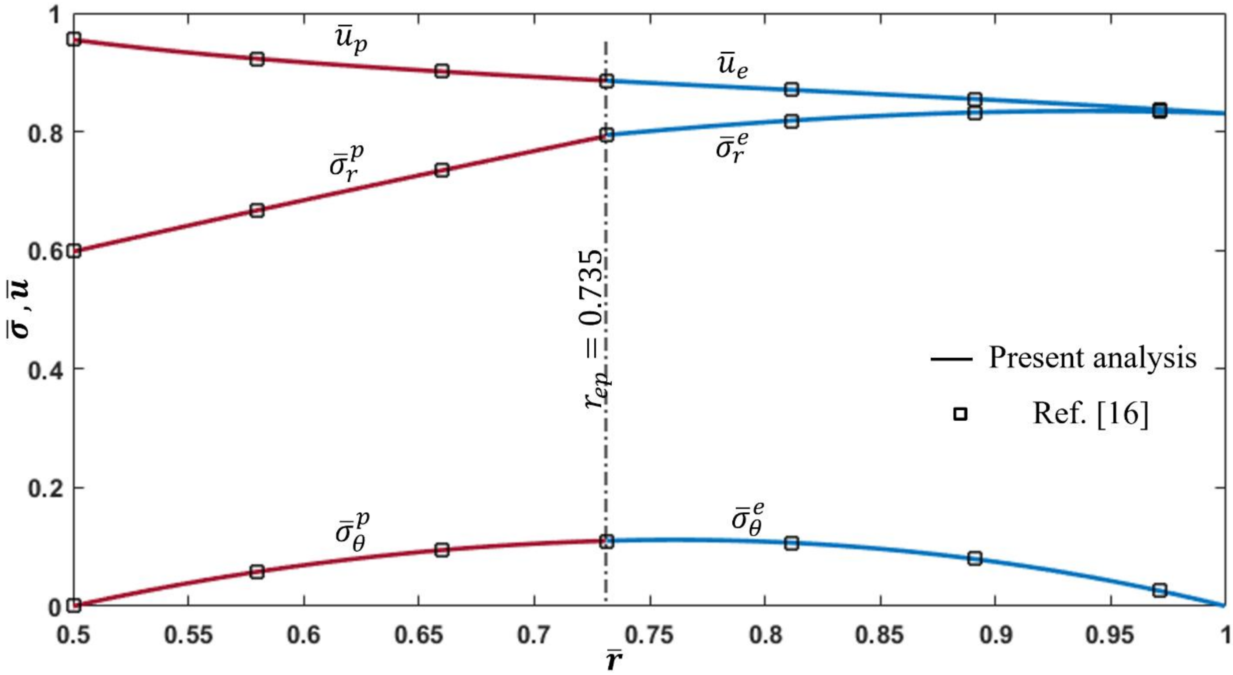

Figure 12 Variation of the radial stress, $\bar{\sigma}_r$, and circumferential stress, $\bar{\sigma}_\theta$, as a function of dimensionless radius, $\bar{r}$, for the angular velocity of $\Omega = 1.34$ and the power parameter of $n = 0.7424$.

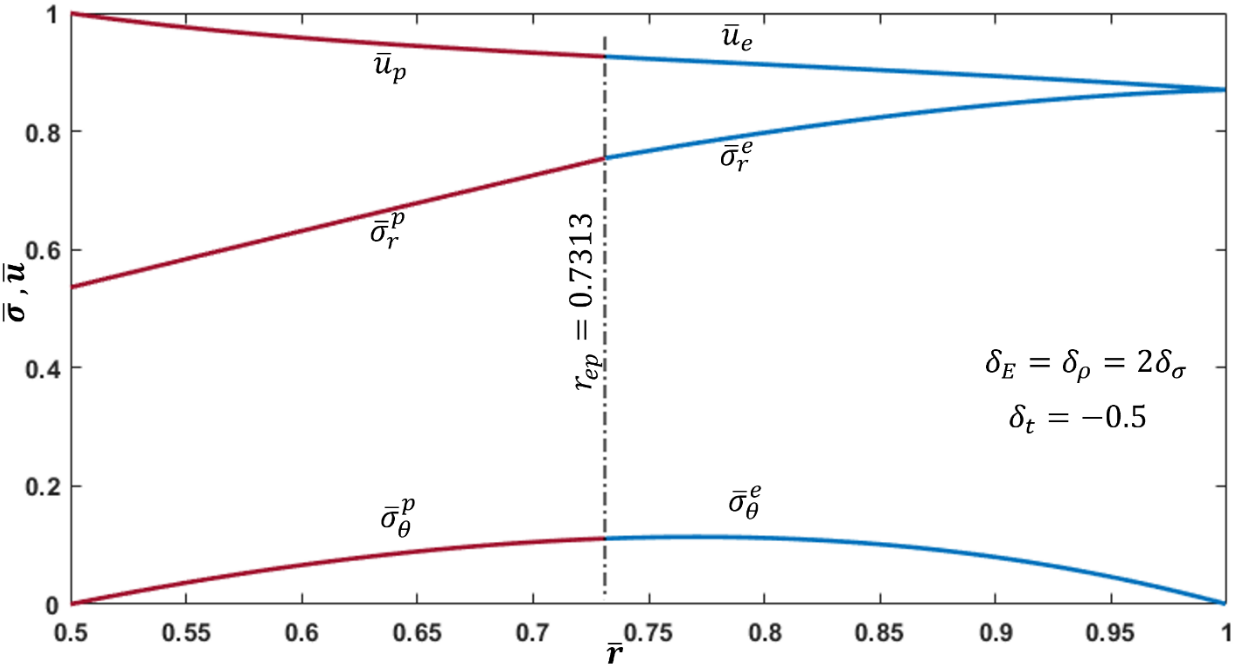

Figure 13 Variation of the radial stress, $\bar{\sigma}_r$, and circumferential stress, $\bar{\sigma}_\theta$, as a function of dimensionless radius, $\bar{r}$, for the angular velocity of $\Omega = 1.39$ and the power parameter of $n = 0.9$.

Table 4 unknown constants $\boldsymbol{C}_{\mathrm{i}}$ and radius of the elastoplastic region $\boldsymbol{r_{ep}}$ for the data presented in figure (13)

$\overline{\boldsymbol{C}}_1$	$\overline{\boldsymbol{C}}_2$	$\overline{\boldsymbol{C}}_3$	$\overline{\boldsymbol{C}}_4$	$\boldsymbol{r_{ep}}$
0.9178	0.0934	-0.2306	-3.0529	0.7313

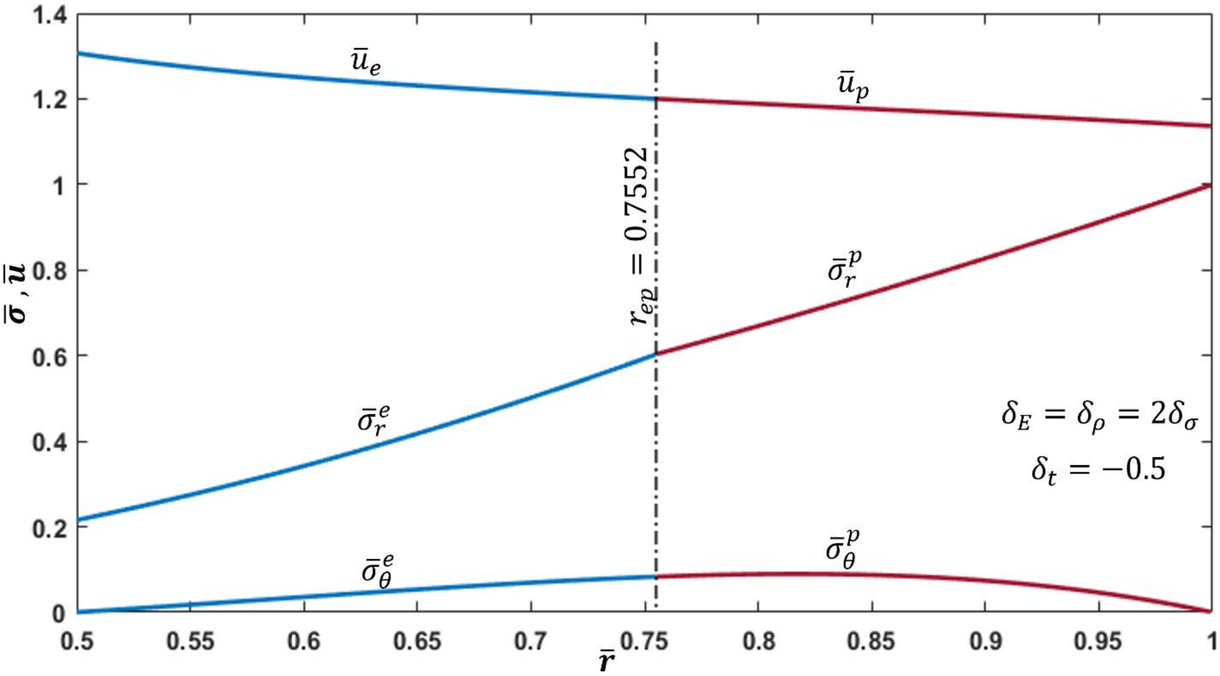

Figure 14 Variation of the radial stress, $\bar{\boldsymbol{\sigma}}_{\boldsymbol{r}}$, and circumferential stress, $\bar{\boldsymbol{\sigma}}_{\boldsymbol{\theta}}$, as a function of dimensionless radius, $\bar{\boldsymbol{r}}$, for the angular velocity of $\boldsymbol{\Omega = 1.46}$ and the power parameter of $\boldsymbol{n = 18}$.

Table 5 unknown constants $\boldsymbol{C}_{\mathrm{i}}$ and radius of the elastoplastic region $\boldsymbol{r_{ep}}$ for the data presented in figure (14)

$\overline{\boldsymbol{C}}_1$	$\overline{\boldsymbol{C}}_2$	$\overline{\boldsymbol{C}}_3$	$\overline{\boldsymbol{C}}_4$	$\boldsymbol{r_{ep}}$
1.2233	0.0227	-0.1524	1.4874	0.7552

Figure (14) shows the progression of the plastic region for a rotating annular disk from the outer radius. As can be seen, for the power parameter of n = 1.8 and angular velocity of Ω =1.46, the boundary of the plastic region extends from the outer radius to the dimensionless radius of r_{ep} = 0.7552. Table (5) shows the unknown constants, C_{i}, in the elastic and plastic regions, as well as the radius of the elastoplastic region r_{ep}.

4 Conclusion

In this paper, in order to investigate the effects of different parameters on the initiation of yielding of a variable-thickness rotating disk made of functionally graded materials, an elastoplastic analytical study based on Tresca's criterion has been carried out. The thickness of the disk cross section, modulus of elasticity, density, and yield stress, are assumed to be exponential functions of radial coordinate. An elastic-perfectly-plastic model has also been used, ignoring strain hardening. The obtained results clearly show the importance of taking variation of the thickness into account. In addition, realizing the fact that the yield point of a homogeneous disk always starts at the inner radius, different states of yielding initiation and the process of expanding the flow of plastic into the rotating disk were researched.

References

[1] U. Gamer, "Tresca’s Yield Condition and the Rotating Disk," *Journal of Applied Mechanics,* vol. 50, no. 3, pp. 676-678, 1983.

[2] U. Gamer, "Elastic-plastic Deformation of the Rotating Solid Disk," *Ingenieur-Archiv,* vol. 54, no. 5, pp. 345-354, 1984.

[3] U. Gamer, "The Elastic-plastic Stress-distribution in the Rotating Annulus and in the Annulus Under External-pressure," in *Zeitschrift Fur Angewandte Mathematik Und Mechanik*, 1984, vol. 64, no. 4: AKADEMIE VERLAG GMBH MUHLENSTRASSE 33-34, D-13187 BERLIN, GERMANY, pp. T126-T128.

[4] U. Gamer, "Stress-distribution in the Rotating Elastic-plastic Disk," *ZEITSCHRIFT FUR ANGEWANDTE MATHEMATIK UND MECHANIK,* vol. 65, no. 4, pp. T136-T137, 1985.

[5] U. Güven, "Elastic-plastic Stresses in a Rotating Annular Disk of Variable Thickness and Variable Density," *International Journal of Mechanical Sciences,* vol. 34, no. 2, pp. 133-138, 1992.

[6] U. Güven, "On the Stresses in an Elastic-plastic Annular Disk of Variable Thickness Under External Pressure," *International Journal of Solids and Structures,* vol. 30, no. 5, pp. 651-658, 1993/01/01/ 1993, https://doi.org/10.1016/0020-7683(93)90027-5.

[7] D. Rees, "Elastic-plastic Stresses in Rotating Discs by von Mises and Tresca," *ZAMM-Journal of Applied Mathematics and Mechanics/Zeitschrift für Angewandte Mathematik und Mechanik: Applied Mathematics and Mechanics,* vol. 79, no. 4, pp. 281-288, 1999, https://doi.org/10.1002/(SICI)1521-4001(199904)79:4<281::AID-ZAMM281>3.0.CO;2-V.

[8] L. You and J. Zhang, "Elastic-plastic Stresses in a Rotating Solid Disk," *International Journal of Mechanical Sciences,* vol. 41, no. 3, pp. 269-282, 1999.

[9] L. You, Y. Tang, J. Zhang, and C. Zheng, "Numerical Analysis of Elastic–plastic Rotating Disks with Arbitrary Variable Thickness and Density," *International Journal of Solids and Structures,* vol. 37, no. 52, pp. 7809-7820, 2000.

[10] Y. Orcan and A. N. Eraslan, "Elastic–plastic Stresses in Linearly Hardening Rotating Solid Disks of Variable Thickness," *Mechanics Research Communications,* vol. 29, no. 4, pp. 269-281, 2002.

[11] A. N. Eraslan and Y. Orcan, "Elastic–plastic Deformation of a Rotating Solid Disk of Exponentially Varying Thickness," *Mechanics of Materials,* vol. 34, no. 7, pp. 423-432, 2002.

[12] A. N. Eraslan and H. Argeso, "Limit Angular Velocities of Variable Thickness Rotating disks," *International Journal of Solids and Structures,* vol. 39, no. 12, pp. 3109-3130, 2002.

[13] F. Vivio and L. Vullo, "Elastic–plastic Analysis of Rotating Disks Having Non-linearly Variable Thickness: Residual Stresses by Overspeeding and Service Stress State Reduction," *Annals of Solid and Structural Mechanics,* vol. 1, no. 2, pp. 87-102, 2010.

[14] H. EkhteraeiToussi and M. RezaeiFarimani, "Elasto-plastic Deformation Analysis of Rotating Disc Beyond Its Limit Speed," *International Journal of Pressure Vessels and Piping*, vol. 89, pp. 170-177, 2012/01/01/ 2012, https://doi.org/10.1016/j.ijpvp.2011.11.001.

[15] B. H. Jahromi, H. Nayeb-Hashemi, and A. Vaziri, "Elasto-plastic Stresses in a Functionally Graded Rotating Disk," *Journal of Engineering Materials and Technology*, vol. 134, no. 2, 2012.

[16] M. Z. Nejad, A. Rastgoo, and A. Hadi, "Exact Elasto-plastic Analysis of Rotating Disks Made of Functionally Graded Materials," *International Journal of Engineering Science*, vol. 85, pp. 47-57, 2014/12/01/ 2014, https://doi.org/10.1016/j.ijengsci.2014.07.009.

[17] E. Lomakin, S. Alexandrov, and Y.-R. Jeng, "Stress and Strain Fields in Rotating Elastic/Plastic Annular Discs," *Archive of Applied Mechanics*, vol. 86, no. 1-2, pp. 235-244, 2016.

[18] A. K. Thawait, L. Sondhi, S. Sanyal, and S. Bhowmick, "Elastic Analysis of Functionally Graded Variable Thickness Rotating Disk by Element Based Material Grading," *Journal of Solid Mechanics*, vol. 9, no. 3, pp. 650-662, 2017. [Online]. Available: https://jsm.arak.iau.ir/article_533193_b892da5f865196adc445b53af0de8db0.pdf.

[19] S. Sharma and S. Yadav, "Numerical Solution of Thermal Elastic-plastic Functionally Graded Thin Rotating Disk with Exponentially Variable Thickness and Variable Density," *Thermal Science*, vol. 23, no. 1, pp. 125-136, 2019, https://doi.org/10.2298/TSCI131001136S.

[20] P. Nayak, S. Bhowmick, and K. N. Saha, "Elasto-plastic Analysis of Thermo-Mechanically Loaded Functionally Graded Disks by an Iterative Variational Method," *Engineering Science and Technology, an International Journal*, vol. 23, no. 1, pp. 42-64, 2020/02/01/ 2020, https://doi.org/10.1016/j.jestch.2019.04.007.

[21] E. Semka, M. Artemov, Y. Babkina, E. Baranovskii, and A. Shashkin, "Mathematical Modeling of Rotating Disk States," in *Journal of Physics: Conference Series*, 2020, vol. 1479, no. 1: IOP Publishing, p. 012122, 10.1088/1742-6596/1479/1/012122.

[22] D. Sharma, R. Kaur, and H. Sharma, "Investigation of Thermo-elastic Characteristics in Functionally Graded Rotating Disk Using Finite Element Method," *Nonlinear Engineering*, vol. 10, no. 1, pp. 312-322, 2021, https://doi.org/10.1515/nleng-2021-0025.

[23] M. Kholdi, S. Saeedi, S. A. Zargar Moradi, A. Loghman, and M. Arefi, "A Successive Approximation Method for Thermo-elasto-plastic Analysis of a Reinforced Functionally Graded Rotating Disc," *Archives of Civil and Mechanical Engineering*, vol. 22, pp. 1-13, 2022, https://doi.org/10.1007/s43452-021-00321-4.

Nomenclature

$\bar{r}$	Radially dimensionless coordinate
a, b	Inner-outer radius of the disk (m)
$\delta_E, \delta_\rho, \delta_\sigma,\ \delta_t$	Physically and geometrically dimensionless constants
$n_E, n_\rho, n_\sigma,\ n_t$	Materially and geometrically dimensionless parameters
$E(E_0)$	Young's modulus (Young's external radius) (Pa)
C_i	Integrating constants
$u(\bar{u})$	Radial displacement (radially dimensionless displacement) (m)
$h(h_0)$	Cross-section thickness (Cross-section thickness of outer radius) (m)
r, θ, z	Coordinates in cylindrical coordinates system

Greek symbols

$\rho(\rho_0)$	Density (density in the outer radius) kgm^{-3}
$\sigma(\bar{\sigma}_i)$	The component of stress (dimensionless stress component) (Pa)
σ_{Y_0}	Yielding stress component in external radius
ν	Poisson's ratio
$\omega(\Omega)$	Angular velocity (dimensionless angular velocity) $(r\ /\ s)$
Ψ	Dimensionless variable depending on Tresca's criterion
ε_i	Strain components